

# Equation of state for shock compressed xenon in the ionization regime: ab initio study

Cong Wang,<sup>1</sup> Yun-Jun Gu,<sup>2</sup> Qi-Feng Chen,<sup>2</sup> Xian-Tu He,<sup>1,3</sup> and Ping Zhang<sup>1,3,\*</sup>

<sup>1</sup>*LCP, Institute of Applied Physics and Computational Mathematics,  
P.O. Box 8009, Beijing 100088, People's Republic of China*

<sup>2</sup>*Laboratory for Shock Wave and Detonation Physics Research,  
Institute of Fluid Physics, P.O. Box 919-102,  
Mianyang, Sichuan, Peoples Republic of China*

<sup>3</sup>*Center for Applied Physics and Technology,  
Peking University, Beijing 100871, People's Republic of China*

## Abstract

Quantum molecular dynamic (QMD) simulations have been applied to study the thermophysical properties of liquid xenon under dynamic compressions. The equation of state (EOS) obtained from QMD calculations are corrected according to Saha equation, and contributions from atomic ionization, which are of predominance in determining the EOS at high temperature and pressure, are considered. For the pressures below 160 GPa, the necessity in accounting for the atomic ionization has been demonstrated by the Hugoniot curve, which shows excellent agreement with previous experimental measurements, and three levels of ionization have been proved to be sufficient at this stage.

PACS numbers: 65.20.De, 64.30.Jk, 31.15.xv

## I. INTRODUCTION

Accurate understandings of the thermodynamic properties of materials under extreme conditions are of great scientific interest<sup>1</sup>. The relative high temperatures (several eV) and densities (several g/cm<sup>3</sup>) produce the so-called “warm dense matter” (WDM), which provides an active research platform by combining the traditional plasma physics and condensed matter physics. WDM usually appears in shock or laser heated solids, inertial confinement fusion, and giant planetary interiors, where simultaneous dissociations, ionizations, and degenerations make modelling of the dynamical, electrical, and optical properties of WDM extremely challenging.

The study of xenon in the warm dense region has long been focused because of the potential applications in power engineering and the significance in astrophysics<sup>2</sup>. Various experimental measurements<sup>3-9</sup> and theoretical models<sup>10-14</sup> have been applied to probe the EOS of xenon. Since the ionization equilibrium are not interfered with the dissociation equilibrium between molecules and atoms, xenon, which is characterized by monoatomic molecule and close shell electronic structure, is particularly suitable for the investigation of the high pressure behavior under extreme conditions. Despite its simple atomic structure, modelling the EOS of xenon under dynamic compression, especially the Hugoniot curve, is an essential issue. For instance, 0-K isotherm, which is important in determining the physical properties of solid xenon under static pressure, has been modelled by augmented-plane-wave (APW) electron band theory method<sup>12</sup>. While, the EOS of xenon under dynamic compression has been calculated through the fluid perturbation theory (FPT), and compared with experimental data<sup>12</sup>. On the other hand, the chemical picture of fluid xenon can be simply described through the concept of plasma physics, deep insight into the shock compressed xenon has been extracted by the self-consistent fluid variational theory (SFVT)<sup>14</sup>.

However, the electronic structure has been convinced to be the key role in determining the thermophysical properties of WMD<sup>15</sup>. Due to the intrinsic approximations of these classical methods, fully quantum mechanical description of xenon under shock compressions still remains to be presented and understood. Meanwhile, QMD simulations, where quantum effects are considered by the combinations of classical molecular dynamics for the ions and density functional theory (DFT) for electrons, have already been proved to be successful in describing WDM<sup>16,17</sup>.

In the present paper, QMD simulations, where free electrons induced by the high temperatures and pressures are considered, have been used to calculate the thermophysical properties of warm dense xenon. The EOS are determined for a wide range of densities and temperatures, and compared with experimental measurements and different theoretical models. The Hugoniot curves, where different levels of ionization are considered, are then derived from the EOS. The rest of the paper is organized as follows. The simulation details are briefly described in Sec. II; Corrections to QMD data and the EOS are presented in Sec. III. Finally, we close our paper with a summary of our main results.

## II. COMPUTATIONAL METHOD

In this work, we have performed simulations for shock compressed xenon by employing the Vienna Ab-initio Simulation Package (VASP), which was developed at the Technical University of Vienna<sup>18,19</sup>.  $N$  atoms in a fixed volume supercell, repeated throughout the space periodically, form the elements of simulations. After introducing Born-Oppenheimer approximation, the thermo-activated electrons are fully quantum mechanically treated through plane-wave, finite-temperature DFT<sup>20</sup>. The electronic states are populated according to the Fermi-Dirac distribution at temperature  $T_e$ . The exchange correlation functional is determined by generalized gradient approximation (GGA) with the parametrization of Perdew-Wang 91<sup>21</sup>. Projector augmented wave (PAW) pseudopotential<sup>22</sup> are used to present the ion-electron interactions. The electronic structure are obtained from a series of given ionic positions, which are subsequently varied according to the forces calculated within the framework of DFT via the Hellmann-Feynman theorem at each molecular dynamics step. The simulations are executed with the isokinetic ensemble (NVT), where the ionic temperature ( $T_i$ ) is controlled by Nosé thermostat<sup>23</sup>, and the system is kept in local thermo-dynamical equilibrium by setting the electron temperature  $T_e$  equal to  $T_i$ .

The bulk of the QMD simulations are performed using  $\Gamma$  point to sample the Brillouin zone in molecular dynamic simulations with the plane-wave cutoff of 600.0 eV, because EOS (pressure and energy) can only be modified within 5% for the selection of higher number of  $\mathbf{k}$  points and larger cutoff energy. A number of 64 atoms is included in the simulation box. To cover typical Hugoniot points with respect to the data obtained from experiments, the densities adopted in our simulations range from 2.965 to 10.0 g/cm<sup>3</sup> and temperatures

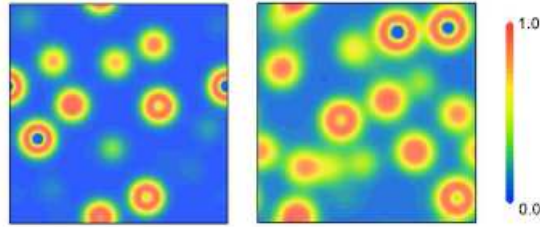


FIG. 1: (Color online) Charge density distribution for different conditions:  $\rho = 5.0 \text{ g/cm}^3$ ,  $T = 1000 \text{ K}$  (left panel); and  $\rho = 9.5 \text{ g/cm}^3$ ,  $T = 40000 \text{ K}$  (right panel).

between 165 and 50000 K. Each density and temperature point is typically simulated for  $4 \sim 6 \text{ ps}$ , and the time step selected for the integrations of atomic motion lies between 0.5 and 2.0 fs with respect to different conditions. Then, the subsequent 1 ps at equilibrium are used to calculate EOS as running averages.

### III. RESULTS AND DISCUSSION

#### A. EFFECTS OF FREE ELECTRONS IN WARM DENSE XENON

Internal energy for shock compressed materials can be expressed as:

$$E_{tot} = E_{ion} + T_{ion} + \int dr V_{ext}(r) n(r) + \frac{1}{2} \int dr V_H(r) n(r) + E_{xc} + T_{electron} + \Delta E_I, \quad (1)$$

where  $E_{ion}$  and  $T_{ion}$  correspond to the interaction energy and the kinetic energy of the bare nuclear. The third term comes from the fixed external potential  $V_{ext}(r)$  (in most cases the potential is due to the classical nuclei), in which the electrons move. The fourth term is the classical electrostatic energy of the electronic density, which can be obtained from the Hartree potential.  $E_{xc}$  and  $T_{electron}$  denote exchange-correlation energy and the kinetic energy of electrons. Finally, the ionization energy is added in the last term, which stands for the energy to generate free electrons and should be seriously considered in the warm dense region. In QMD simulations, the last term is excluded, and the simulated results should be

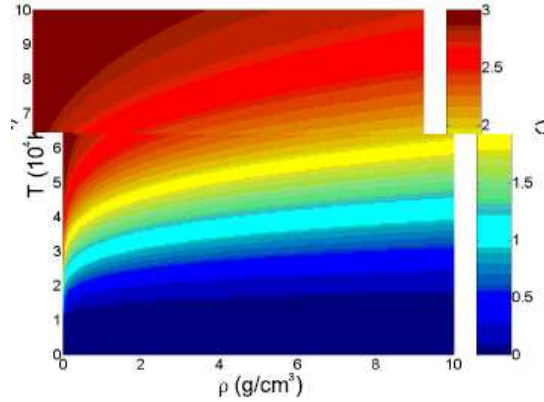


FIG. 2: (Color online) The ionized electron number as a function of the density and temperature.

corrected. The total internal energy is then expressed as:

$$E_{tot} = E_{QMD} + N \sum_i \alpha_i E_i,$$

where  $N$  is the total number of atoms for the present system, and  $\alpha_i$  is the  $i$ -th level ionization degree,  $E_i$  is the energy required to remove  $i$  electrons from a neutral atom, creating an  $i$ -level ion. Here,  $E_i$  equals to  $\sum_i \Delta \epsilon_i$ , and  $\Delta \epsilon_i$  is the  $i$ -th ionization energy.

Free electrons can be introduced at high temperatures and pressures by subsequent ionization of atoms. The ionization process can be revealed from the change of the charge density distribution with increasing density and temperature, as shown in Fig. 1. In lower density and temperature region, the localization of electrons represents the atomic fluid. While, metallic behaviors of fluid xenon are indicated by delocalization of electrons, which can be attributed to the thermo-activation of electronic states. Similar phenomena have already been found for another noble gas helium<sup>24</sup> and the expanded fluid alkali metal Li<sup>16</sup>.

Although ionizations of electrons can be qualitatively described in the framework of finite-temperature DFT, contributions to pressure from noninteracting electrons are still lacking. Thus, the total pressure should be corrected as:

$$P_{tot} = P_{QMD} + \sum_i i \alpha_i \frac{\rho k_B T}{m}, \quad (2)$$

where  $m$  presents the mass of xenon atom. The density and temperature are denoted by  $\rho$  and  $T$  respectively, and  $k_B$  stands for Boltzmann constant.  $E_{QMD}$  and  $P_{QMD}$  are obtained

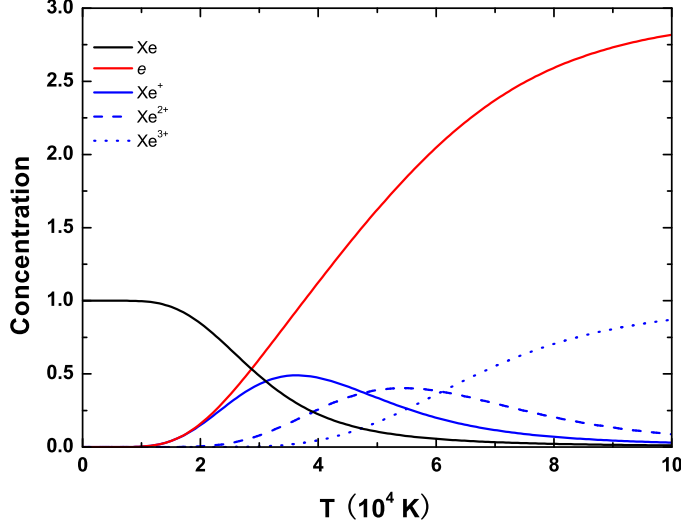


FIG. 3: (Color online) Component of plasma xenon as a function of temperature at  $\rho = 6.0 \text{ g/cm}^3$ .

from VASP. Since, it is difficult to quantify the ionization degree for  $i$ -th level from direct QMD results, as an alternative selection, we use Saha equation to verify the degree of each ionization level:

$$\frac{n_{i+1}n_e}{n_i} = \frac{2\Omega}{\lambda^3} \frac{g_{i+1}}{g_i} \exp\left(-\frac{\Delta \epsilon_i}{k_B T}\right), \quad (3)$$

$$\lambda = \sqrt{\frac{h^2}{2\pi m_e k_B T}}, \quad (4)$$

where  $n_i$  is the density of atoms in the  $i$ -th state of ionization, that is with  $i$  electrons removed,  $g_i$  is the degeneracy of states for the  $i$ -ions,  $n_e$  is the electron density,  $\lambda$  is the thermal de Broglie wavelength of an electron,  $m_e$  is the electron mass, and  $\Omega$  is the volume of the supercell. Here,  $\alpha_i$  equals to  $n_i\Omega/N$ . Similar approximations have already been used to study the EOS of liquid deuterium under shock compressions<sup>25</sup>, where soften behavior of the Hugoniot curve has been found at high pressure, and the simulated results are consist with available experiments.

In the present work, three levels of ionization have been considered (the relative ionization energies are 12.1, 21.2, and 32.1 eV respectively), and the relative electron number (equals to  $\sum_i i\alpha_i$ ) as a function of density and temperature are labelled in Fig. 2. Xenon under extreme conditions is considered to be partially ionized plasma, where ionization equilibrium:  $\text{Xe}^{(i-1)+} \rightleftharpoons \text{Xe}^{i+} + e$ , stands for the changes in the electronic structure under high temperatures and pressures. Three levels of atomic ionization have been taken into account

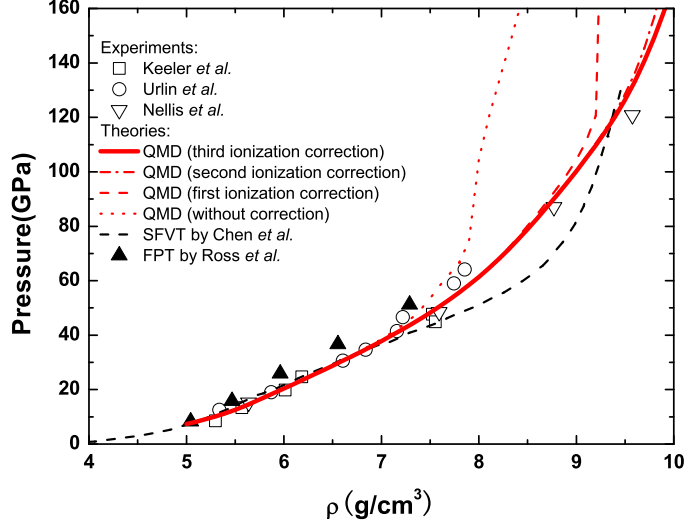


FIG. 4: (Color online) Hugoniot for shocked liquid xenon are compared with previous experimental<sup>3,4,7,8</sup> and theoretical results<sup>12,14</sup>. Specially, the results, which are corrected according to different ionization level, are also provided.

in the present calculations. As an example, the composition for density of 6.0 g/cm<sup>3</sup> is plotted in Fig. 3. The fraction of charged ions Xe<sup>+</sup>, and Xe<sup>2+</sup> increase to maximum, then decrease, and the number of Xe<sup>3+</sup> and electrons increase monotonously with temperature, while the number of neutral atom Xe decrease with the increase of temperature. The Hugoniot of shocked compressed liquid xenon can be effectively modified with the consideration of atomic ionizations, and the detailed discussion can be found in Sec. III B.

## B. THE EQUATION OF STATE

Let us turn now to see the Hugoniot by investigating the corrected EOS of warm dense xenon. Following Lenosky *et al.*, Beule *et al.*, and Holst *et al.*<sup>26–28</sup>, smooth functions are used to fit the internal energies and pressures by expansions in terms of density (g/cm<sup>3</sup>) and temperature (10<sup>3</sup> K). The corrected QMD data for internal energy (eV/atom) can be expanded as follows:

$$E = \sum_{i=0}^2 A_i(T) \rho^i, \quad (5)$$

$$A_i(T) = a_{i0} \exp\left[-\left(\frac{T - a_{i1}}{a_{i2}}\right)^2\right] + a_{i3} + a_{i4}T. \quad (6)$$

The total pressure given in GPa can be similarly expanded as:

$$P = \sum_{j=0}^2 B_j(T) \rho^j, \quad (7)$$

$$B_j(T) = b_{j0} \exp[-(\frac{T - b_{j1}}{b_{j2}})^2] + b_{j3} + b_{j4}T. \quad (8)$$

The expansion coefficients  $a_{ik}$  and  $b_{jk}$  for  $E$  and  $P$  (accuracy better than 5%) are summarized in Tab. I and Tab. II, respectively.

TABLE I: Coefficients  $a_{ik}$  in expansion for the internal energy  $E$ .

$i$	$a_{i0}$	$a_{i1}$	$a_{i2}$	$a_{i3}$	$a_{i4}$
0	57.3976	-17.3142	28.2460	-38.0864	1.7336
1	11.2512	13.0002	-67.2259	-11.4532	0.0057
2	-0.7180	41.0407	73.9168	0.6057	0.0060

TABLE II: Coefficients  $b_{jk}$  in expansion for the total pressure  $P$ .

$j$	$b_{j0}$	$b_{j1}$	$b_{j2}$	$b_{j3}$	$b_{j4}$
0	-38.9090	-15.8020	72.3514	63.7065	-0.0607
1	0.3299	26.0136	-5.7763	-12.5064	-0.0294
2	0.7302	1.0722	19.2058	0.9256	0.0441

A crucial measurement of the EOS data of xenon under shock conditions is the Hugoniot, which can be derived from the following equation:

$$(E_0 - E_1) + \frac{1}{2}(V_0 - V_1)(P_0 + P_1) = 0, \quad (9)$$

where  $E$  is the internal energy,  $P$  is the pressure,  $V$  is the volume, and the subscripts 0 and 1 denote the initial and shocked state, respectively. The Hugoniot relation, which describes the locus of points in  $(E, P, V)$ -space, follows from conservation of mass, momentum, and energy for an isolated system compressed by a pusher at a constant velocity. In our simulations, the initial density  $\rho_0$  is 2.965 g/cm<sup>3</sup>, the relative internal energy  $E_0=0.01$  eV/atom at  $T_0=165$  K. The initial pressure  $P_0$  of the start point on the Hugoniot can be approximated to be zero compared to high pressure of shocked states.



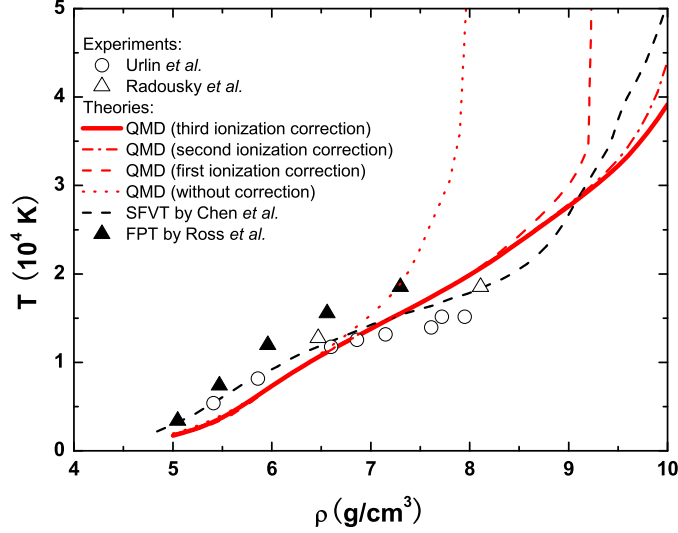


FIG. 5: (Color online) Temperature is labelled as a function of density along the Hugoniot. Previous experimental<sup>8,10</sup> and theoretical<sup>12,14</sup> results are also included.

The Hugoniot curve, where results from our simulations and previous predictions from both experiments and theories are labelled for comparison, is shown in Fig. 4. In order to clarify the influence of atomic ionization, results from direct QMD simulations and those corrected by Saha equation are also provided in the present work. Agreements can be found between experimental measurements and the uncorrected QMD results only below 70 GPa. However, at higher pressures ( $P > 70$  GPa), the uncorrected Hugoniot curve shows an abrupt increase, which suggests a stiff behavior, and unphysical results are obtained here because of the ignorance of atomic ionization. Considerable softening of the Hugoniot can be achieved by the corrected QMD calculations, and reliable results are gradually revealed through accounting for the first, second, and third level of ionization. Here, the wide-range EOS for shock compressed liquid xenon can be well described by the corrected QMD simulations (with the consideration of three levels of ionization) below 160 GPa, where good agreements are detected between our simulation results and experiments<sup>3,4,7,8</sup>. Theoretically, no Hugoniot points by previous FPT method<sup>12</sup> are available to be used to compare with experiments at pressures higher than 60 GPa, and the Hugoniot curve from SFVT<sup>14</sup> seems to be inconsistent with the results from Nellis *et al.*<sup>4</sup>.

Temperature, which is focused as one of the most important parameters in experiments, is difficult to be measured because of the uncertainty in determining the optical-intensity loss

for ultraviolet part of the spectrum in adiabatic or isentropic shock compressions, especially for the temperature exceeding 20000 K. QMD simulations provide powerful tools to predict shock temperature. Our calculated Hugoniot temperature is shown in Fig. 5 as a function of the density. For comparison, the previous simulated (FPT<sup>12</sup> and SFVT<sup>14</sup>) and experimental (by Radousky *et al.*<sup>10</sup> and Urlin *et al.*<sup>8</sup>) results are also shown in Fig. 5. One can find that the present calculated temperatures for the direct and corrected QMD simulations begin to depart at about 10000 K (the respective density is 6.5 g/cm<sup>3</sup>), which highlights the start point of ionization on the Hugoniot. Discontinuous change in temperature, which is similar to the behavior of Hugoniot, has been found in the direct QMD simulation results, while, smooth variations of temperature along the Hugoniot are predicted by the corrected simulation results. The corrected shock temperatures are accordant with the available experiments.

#### IV. CONCLUSION

In summary, QMD simulations, where contributions from ionized electrons are taken into account, are introduced to investigate the EOS of shock compressed liquid xenon, and ionization equilibrium:  $\text{Xe}^{(i-1)+} \rightleftharpoons \text{Xe}^{i+} + e$  is described by Saha equation. Here, three levels of ionization are considered, and it has been demonstrated that the accuracy of the calculated EOS can be effectively improved through the present approximations. The corrected EOS data are fitted by smooth functions, from which Hugoniot curve are then derived. Good agreements have been achieved between our calculated results and those from experimental measurements.

#### Acknowledgments

This work was partially supported by the National High-Tech ICF Committee of China.

---

\* Corresponding author; zhang\_ping@iapcm.ac.cn

<sup>1</sup> R. Ernstorfer, M. Harb, C. T. Hebeisen, G. Sciaini, T. Dartigalongue, R. J. D. Miller, *Science*, **323**, 1033 (2009).

- <sup>2</sup> R. Paul Drake, *High Energy Density Physics: Fundamental Inertial Fusion, and Experimental Astrophysics*, (Springer, Berlin, 2006), p.5.
- <sup>3</sup> R. N. Keeler, M. van Thiel, and B. J. Alder, *Physica (Utrecht)*, **31**, 1437 (1965).
- <sup>4</sup> W. J. Nellis, M. van Thiel, and A. C. Mitchell, *Phys. Rev. Lett.*, **48**, 816 (1982).
- <sup>5</sup> V. E. Fortov, A. A. Leontev, A. N. Dremin, and V. K. Gryaznov, *Zh. Eksp. Teor. Fiz.*, **71**, 225 (1976) (in Russian).
- <sup>6</sup> V. K. Gryaznov, M. V. Zhernokletov, V. N. Zubarev, I. L. Iosilevsky, and V. E. Fortov, *Zh. Eksp. Teor. Fiz.*, **78**, 573 (1980) (in Russian).
- <sup>7</sup> V. D. Urlin, M. A. Mochalov, and O. L. Mikhailova, *Mat. Model.*, **3**, 42 (1991) (in Russian).
- <sup>8</sup> V. D. Urlin, M. A. Mochalov, and O. L. Mikhailova, *High Press. Res.*, **8**, 595 (1991).
- <sup>9</sup> M. I. Eremets, E. A. Gregoryanz, V. V. Struzhkin, H. Mao, R. J. Hemley, N. Mulders, and N. M. Zimmerman, *Phys. Rev. Lett.*, **85**, 2797 (2000).
- <sup>10</sup> H. B. Radousky and M. Ross, *Phys. Lett. A*, **129**, 43 (1988).
- <sup>11</sup> S. Kuhlbrodt, R. Redmer, H. Reinholz, G. Ropke, B. Holst, V. B. Mintsev, V. K. Grayaznov, N. S. Shilkin, and V. E. Fortov, *Contrib. Plasma Phys.*, **45**, 61 (2005).
- <sup>12</sup> M. Ross and A. K. McMahan, *Phys. Rev. B*, **21**, 1658 (1980).
- <sup>13</sup> V. Schwarz, H. Juranek, and R. Redmer, *Phys. Chem. Chem. Phys.*, **7**, 1990 (2005).
- <sup>14</sup> Q. F. Chen, L. C. Cai, Y. J. Gu, and Y. Gu, *Phys. Rev. E*, **79**, 016409 (2009).
- <sup>15</sup> C. Wang and P. Zhang, *J. Chem. Phys.*, **132**, 154307 (2010).
- <sup>16</sup> A. Kietzmann, R. Redmer, M. P. Desjarlais, and T. R. Mattsson, *Phys. Rev. Lett.*, **101** 070401 (2008).
- <sup>17</sup> W. Lorenzen, B. Holst, and R. Redmer, *Phys. Rev. Lett.*, **102** 115701 (2009).
- <sup>18</sup> G. Kresse and J. Hafner, *Phys. Rev. B*, **47** R558 (1993).
- <sup>19</sup> G. Kresse and J. Furthmüller. *Phys. Rev. B*, **54** 11 169 (1996).
- <sup>20</sup> T. Lenosky, S. Bickham, J. Kress, and L. Collins, *Phys. Rev. B*, **61** 1 (2000).
- <sup>21</sup> J. P. Perdew, *Electronic Structure of Solids* (Akademie Verlag, Berlin, 1991).
- <sup>22</sup> P. E. Blöchl, *Phys. Rev. B*, **50** 17953 (1994).
- <sup>23</sup> S. Nosé, *J. Chem. Phys.*, **81** 511 (1984).
- <sup>24</sup> A. Kietzmann, B. Holst, R. Redmer, M. P. Desjarlais, and T. R. Mattsson, *Phys. Rev. Lett.*, **98** 190602 (2007).
- <sup>25</sup> C. Wang, X. T. He, and P. Zhang, arXiv:1004.1281.

- <sup>26</sup> T. J. Lenosky, J. D. Kress, and L. A. Collins, Phys. Rev. B, **56** 5164 (1997).
- <sup>27</sup> D. Beule, W. Ebeling, A. Föster, H. Juranek, S. Nagel, R. Redmer, and G. Röpke, Phys. Rev. B, **59** 14177 (1999).
- <sup>28</sup> B. Holst, R. Redmer, and M. P. Desjarlais, Phys. Rev. B, **77** 184201 (2008).